Computational Modeling of Failure Patterns of Glass Panels with Imperfections Subjected to Air Blast

Hossein Ataei[1], James C. Anderson[2]

[1,2]Sonny Astani Department of Civil and Environmental Engineering
Viterbi School of Engineering, University of Southern California (USC)
3620 S. Vermont Ave., Kaprielian Hall Room 210, Los Angeles, CA, 90089, USA
[1]ataei@usc.edu; [2]jamesa@usc.edu

***Abstract*-Glass fragments are a prime source of injury to occupants of buildings subjected to explosive events during which window glass breaks into either flying shards (annealed glass windows) or fragments (fully tempered glass). These account for injuries ranging from minor cuts to severe wounds. A successful blast-resistant glazing design requires balancing of the safety and security of the window panels with physical appearance and cost-effectiveness. Moreover, it should consider the principles of a reasonable degree of protection against explosive threats based on the proposed level of security and previous lessons learned.**

In this paper, explicit finite element method (FEM) with is used for modeling the window failure and investigate the failure patterns of annealed and fully tempered glass windows panels with embedded imperfections across the panel. For this purpose, the element-removal technique is utilized in accordance with the fracture micromechanics' principles and the brittle failure criteria of displacements; strains and stresses. The results of the analysis demonstrate that the response of the conventionally-framed window panels to blast loading cases depends upon the glazing technologies; blast load intensities; the glass types; and the location of imperfections.

Through the application of element removal technique and stress redistributions at each infinitesimal time increment, the results of this paper further demonstrates that the existence of glass imperfections in the window panels will make them more vulnerable against the air blast overpressures for both annealed and fully-tempered glass panel cases: For fully tempered glass panels, the vulnerability arises from greater stress concentrations at the location of glass defects as well as higher brittleness of the panel itself when compared to the annealed glass panels.

The results of this study show that the existence of defects along the edges will help in redistribution of the stresses in a way that the yield lines will pass through these imperfection locations. The general failure pattern for defective annealed glass panels subjected to small intensity air blast will be very similar to the failure pattern of homogeneous window panels yet with a faster pace. However, when subjected to a higher intensity air blast, the severity of the load will cause excessive rotation angles in the panel and subsequent computational divergence and instability. The panel failure will occur much faster and with different patterns compared to the case of annealed glass panels subjected to smaller intensity air blasts.

Keywords- Glass; Air Blast; Safety; Window Panels; Fracture Mechanics; Crack Propagation

I. INTRODUCTION

Extreme loading on various glazing systems, during an air blast, results in shattering of glass panels into smaller pieces which fly at very high velocities. Due to the high-impact, low-frequency nature of the blast waves and potential risk to the occupants, strict design criteria should be put in place for design of the building envelope and structural glazing systems. In the computer models that are used in this study, the blast pulse is assumed to have a triangular shape in which the overpressure rises instantaneously to its peak value (peak pressure) and has a linear decay back to zero (atmospheric pressure) in a very short period of time (milliseconds).

In this paper, conventionally-framed annealed glass (AG) and fully tempered (FT) window panels of 50 cm x 75 cm (20" x 30") are modeled and analyzed. Due to the high velocity of the air blast wave, the building occupants have little time to prepare for the arrival of the wave which is normally in the order of milliseconds. Therefore the existing structure must provide a measure of protection. Each window panel is studied for the effects of two different air blast loadings: (i) Smaller intensity air blast due to 100 Lbs of TNT with 30.5 meters (100 ft) as the explosion stand-off distance and (ii) Higher intensity air blast due to 1000 Lbs of TNT with an explosion stand-off distance of 30.5 meters (100 ft). The stand-off distance (100 ft) is selected to be the same for both loading cases which, according to the Defense Threat Reduction Agency guidelines, will cause severe wounds and casualties by flying glass shards. During the course of this study, further investigations are also made on the blast loading intensity effects by applying a very high intensity air blast load (5000 Lbs of TNT at 100 ft) to model the glazing system responses and fracture patterns. However, due to the extremely high blast overpressure in this case, the failure mode of the proposed glazing systems was mostly dominated by the intensity of the load itself rather than the effects of the imperfection location or types.

DOI: 10.5963/AMSA0303002

Given the weight of explosive (*W*) and stand-off distances (*R*) for each blast loading intensity and assuming the angle of attack (α) is zero in order to have the highest possible exposure of the glass window panels to the air blast waves for the purposes of examining and investigating the maximum vulnerability and hazard assessment levels, the blast load characteristics of the Peak pressure (P_r); Reflected impulse (i_r) and the Load duration (t_0) are summarized in Table 1 (below). These data are calculated using the "A.T. Blast" software and "Defense Threat Reduction Agency Manuals".

TABLE 1 BLAST LOADING CHARACTERISTICS

W (Kg)	R (m)	i_r (Pa . msec)	P_r (Pa)	t_0 (msec)
45.0	30.5	2.50×10^5	3.98×10^4	12.55
453.5	30.5	1.25×10^6	1.65×10^5	15.12

II. MODEL MATERIAL PROPERTIES

Trawinsky E. et al., (2004) [1] show that more than 80% of human casualties during an air blast event are associated with the failure of window glass panels or curtain walls. Subjected to air blast overpressure, window glass panels break into high-velocity flying shards or fragments that shatter into the offices or residential occupancies causing severe wounds, cuts or even death to the building occupants as these glass fragments can fly and reach large distances. According to Norville H.S. et al. (1999) [2], in 1995 Oklahoma City terrorist bombing event, 198 people who were in buildings within a radius of 970 meters suffered from direct glass-related injuries caused by the flying glass shards.

Annealed Glass (AG) is the most common type of glass that is used in conventional construction and building envelope systems. Subjected to an air blast, it fractures in irregular patterns (with aspect ratios that can reach as high as 10) leading to sharp glass shards that cause injuries to the building occupants varying from minor cuts to severe wounds [GSA Standard Test Methods]. Fully Tempered (FT) glass is made by controlling uniform heating (up to 680^{o}C) and rapid cooling of the annealed glass (AG). The outer surfaces cool and harden before the inner core and therefore it gives the FT panels more hardening and about four times more strength of the annealed glass panels. Furthermore, Johnson N.F. (2006) [3] indicated that the mode of failure and shattering pattern for the fully-tempered panels is to fracture into numerous smaller fragment pieces as opposed to the irregular shards of the annealed glass.

The window panel, in this paper, is modeled using two different types of glazing materials: (1) Annealed Glass (AG) with 6.0 mm (1/4") thickness and (2) Fully Tempered (FT) glass with the thickness of 7.5 mm (0.3"). The types and the properties of the model materials are summarized in Table 2.

TABLE 2 GLAZING MATERIAL PROPERTIES

Glazing Material	Elastic Modulus (GPa)	Poisson's Ratio	Density (kg/m^3)	Fracture Strength (MPa)
Annealed Glass	69	0.22	2491.19	27.58
Fully Tempered Glass	69	0.22	2491.19	110.32

Glass failure stresses can vary significantly even among the glass samples that come from the same lot. The damage accumulation factor; glass age; the non-homogeneity location and shape of the imperfection can negatively affect the actual failure strength of glass panels. Therefore, Ataei H., Anderson J.C., (2013) [4] addressed the necessity of developing the flying glass injury models, the non-homogeneity of structural glass panels need to be further investigated. The presented models in this paper address the crack propagation patterns across the window for a more accurate and comprehensive evaluation of the potential hazard level of each case on the building occupants' safety and security.

III. EXPLICIT FINITE ELEMENT ANALYSIS AND MESH PROPERTIES

Considering the high-speed short-duration nature of the air blasts, explicit dynamic methods are usually used to model and solve the problems involving such loads. According to Belytscheko et al., (2005) [5], in these methods a global tangent stiffness matrix is not required. However, Ataei et al., (2007) [6] mentioned that a stability limit, which technically is a small time increment that is independent of the type and duration of the loading, is required. The stability limit, therefore, solely depends on the highest natural frequency of the model ($\omega_{\max}$) and the fraction of critical damping ($\xi_{\max}$) in the mode with the highest frequency as per the Eq. (1) below as per ABAQUS User's Manual, (2011) [7]:

$$\Delta t_{stability} \le \frac{2}{\omega_{\max}}\left(\sqrt{1+\xi_{\max}{}^2}-\xi_{\max}\right) \quad (1)$$

DOI: 10.5963/AMSA0303002

In addition, Eq. (2) represents a more conservative and practical method also exists to calculate the stability limit of the explicit analysis based on the smallest element length in the mesh (L_{min}) and the dilatational wave speed of the material (c_d) as per ABAQUS User's Manual, (2011) [7]:

$$\Delta t_{stability} \approx \frac{L_{\min}}{c_d} \tag{2}$$

As the material yields, the wave speed reduces and hence, the stability limit takes larger values which will equally result in faster computational convergence after yielding according to Belytscheko et al., (2005) [5]. Larger element sizes will increase the stability limit; however, finer mesh sizes are often necessary to obtain more accurate analysis results (Belytscheko et al., (2005) [5]). The best approach is, therefore, as stated by Ataei H, Anderson J.C., (2012) [8] is to have a fine mesh that is as uniform as possible to obtain the highest possible stability limit.

In this paper, in order to study the crack propagation patterns across defective glass panels, a very fine and uniform initial mesh that consists of square 4-noded shell elements is employed to model the entire window panel as a 3-dimensional deformable shell across the window panel thickness, as shown in Fig. 1.

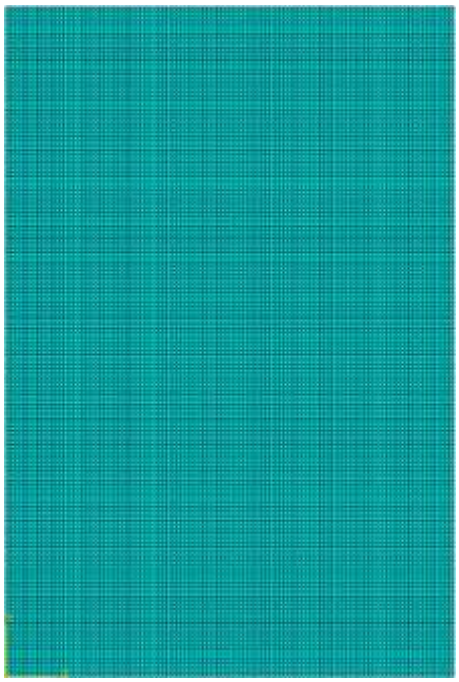

Fig. 1 The initial fine mesh size for modeling 50cm x 75cm glass window panels

The elements in the mesh have dimensions of 1 cm x 1 cm along the Plate Thickness which is in compliance with the ASTM's *United Dimension Requirement* as illustrated in ASTM F1642-04 (2010) [9]. According to this requirement, the sum of the length, width and thickness of the elements in the mesh should not be less than 1" or else, the glass fragments are considered as "glass dust". Total number of elements for the studied window panel of (20" x 30") is 3750 elements. This number, however, was increased to the 15,000 elements through several iterations to further refine the mesh in order to achieve higher precision in modeling the glass failure patterns. As the crack propagates further and the failed elements in the mesh get removed from the panel geometry, re-meshing is automatically performed for the newly-created geometry at each infinitesimal time increment.

The accelerations at the beginning of the current time increment (t) are calculated as per Eq. (3) [7]:

$$\ddot{u}]_{(t)} = (M)^{-1}.(P-I)]_{(t)} \tag{3}$$

Where (M) is the Mass Matrix; (P) is the external applied forces and (I) is the internal element forces. Since the acceleration values of any node are determined completely by its mass and the net force acting on the node, the nodal computations are very inexpensive by using this method.

As illustrated in Eq. (4), the accelerations are integrated through time by applying the central difference rule to calculate the change in velocities. The calculated change in velocity is added to the velocity from the middle of the previous infinitesimal time increment to determine the velocities at the middle of the current increment [7]:

DOI: 10.5963/AMSA0303002

$$\dot{u}]_{(t+\frac{\Delta t}{2})} = \dot{u}]_{(t-\frac{\Delta t}{2})} + \frac{\left(\Delta t]_{(t+\Delta t)} + \Delta t]_{(t)}\right)}{2} \ddot{u}]_{(t)} \tag{4}$$

The velocities are integrated through time and added to the displacements at the beginning of the increment to find the displacements at the end of each time increment as shown in Eq. (5) [7]:

$$u]_{(t+\Delta t)} = u]_{(t)} + \Delta t]_{(t+\Delta t)} \dot{u}]_{(t+\frac{\Delta t}{2})} \tag{5}$$

By having the incremental strain rate ($\dot{\varepsilon}$), the element strain increments ($d\varepsilon$) are calculated, and, by applying material constitutive relationships (element stiffness), the element stresses (σ) are computed and consequently, the internal forces matrix for $t + \Delta t$ is therefore assembled and computed as per Eq. (6).

$$\sigma_{(t+\Delta t)} = f\left(\sigma_{(t)}, d\varepsilon\right) \tag{6}$$

IV. YIELD LINE ANALYSIS OF RECTANGULAR WINDOW PANELS

Limit analysis of rectangular plates or slabs is commonly known as "Yield Line Theory". This concept was introduced in Denmark by Ingerslev (1923) during the period of 1920-1922 [10]. The first summary of this work in English was introduced by Hognestad in 1953 [11]. Since then, it has found considerable application in for the strength design of concrete slabs which can be considered as flat plates.

The fracture pattern of rectangular window panels with (*a* x *b*) dimensions at which *a* is the shorter dimension is demonstrated in Fig. 2:

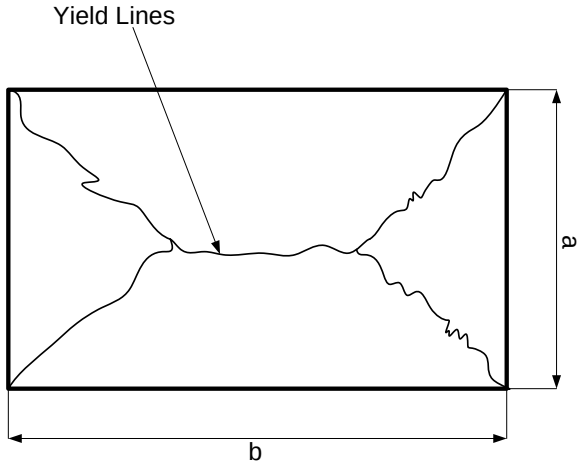

Fig. 2 Theoretical yield-line pattern of rectangular window panels at failure

For a rectangular window panel subjected to uniform blast pressure of (*w*) and simply-supported (conventional framing) along its four edges, the maximum moment is obtained through Eq. (7) according to Nawy E.G., (2000) [12]:

$$M = \frac{wa^2}{24}\left[\sqrt{3+\left(\frac{a}{b}\right)^2} - \frac{a}{b}\right]^2 \tag{7}$$

Therefore, Reddy J.N., (2006) [13] indicated that by having the ultimate strength of each window panel, the breakage pressure values for each window that make the cracks start and propagate afterwards can be calculated. As summarized in Table 3, based on the yield line analysis of simply supported glazing systems, the amount of blast overpressure that makes each of the window panel models fail can be calculated. Moreover, it can be determined whether the breakage happens in the window panels.

However, the yield-line analysis only estimates the ultimate failure load on the panel and does not provide insight on the exact time at which the crack initiates; the crack propagation time histories or on its propagation patterns across the panel versus time. This is mainly due to highly dynamic nature of crack propagation problems and brittle failure analysis methodologies [8].

Park and Gamble (2000) [14] have recommended that for a uniformly loaded rectangular slab with all edges supported a good simplifying approximation is to assume that the positive moment yield lines enter the corners of the slab a 45 degrees to

DOI: 10.5963/AMSA0303002

the edges. They note that the estimated ultimate load may be higher than given by a more exact and more complicated equation but the difference should not be large if the longer side is less than twice the shorter side. Application of this condition results in the theoretical yield lines that are highlighted by red lines in Figs. 3-5 and Figs. 9-11.

TABLE 3 YIELD LINE ANALYSIS OF CONVENTIONAL 50CM X 75CM WINDOW PANELS

		Annealed Glass (50 cm x 75 cm)	Fully-Tempered Glass (50 cm x 75 cm)
45 Kg TNT at 30.5 m	Max Pressure (Pa)	39782.77	39782.77
	Failure Pressure (Pa)	7550.00	47301.35
	Breakage Happens	*Yes*	*No*
453.5 Kg TNT at 30.5 m	Max Pressure (Pa)	165267.40	165267.40
	Failure Pressure (Pa)	7550.00	47301.35
	Breakage Happens	*Yes*	*Yes*

V. DYNAMIC FINITE ELEMENT ANALYSIS OF GLASS BRITTLE FAILURE

In order to precisely capture the behavior of both homogeneous and non-homogeneous window panels that are subjected to small and higher intensity air blast, an infinitesimal time increment of 0.0125 msec (0.0000125 sec) is adopted to advance the state of the model in dynamic explicit analysis. During the analysis, the elements that reach their local failure criteria (stress; strain and crack-tip displacement) are removed from the mesh as well as from the panel geometry before the re-meshing of the whole model and its advancement to the next timeframe for re-computation of stress; strain; reaction forces and crack-tip opening values. The dynamic element deletion sequence, henceforth, is visualized as crack propagation path for investigating the effects of glass imperfections on brittle failure patterns of window glass panels.

The fracture patterns of annealed and fully-tempered glass panels are modeled with "*BRITTLE FAILURE" in ABAQUS that internally uses both "*BRITTLE CRACKING" and "*BRITTLE SHEAR" features for brittle cracking and failure analysis. The maximum stress criterion is utilized and included to identify the glass failure. This criterion states that failure in the glass panels occurs when the maximum principle stresses in the two dimensional coordinate system, (σ_1, σ_2), reach either of the maximum uniaxial tension (σ_t) or compression strength (σ_c) values of the glass.

The Brittle Cracking with "type=displacement" in ABAQUS uses the ultimate tensile failure strength of the glass panels as well as the post-cracking tensile stress and crack opening displacements to model the post-crack stress-displacement relationship. The Brittle Shear option with Retention Factor defines the shear stress-post-crack displacement relationships for the panels and finally the Brittle Failure option defines the type of cracking behavior across the panel with maximum allowable post-crack displacement in order for the crack to nucleate and propagate using the element deletion technique.

The American standards (ASTM E2461) [15] and Canadian standards (CAN/CGSB-12.20-M89) [16] limit the allowable maximum fracture stress for annealed glass to 25 MPa (3.63 ksi) in the center of the pane and 20 MPa (2.90 ksi) on the edges. For fully tempered glass, however, both standards suggest the allowable stress be no greater than 100 MPa (14.50 ksi) in the window panel center. More accurate guidelines limit the glass deflection to the least of either span length divided by 175 or to 3/4" (whichever is less). Moreover, the shock tube experiments performed by Kumar and Shukla (2011) [17] propose an allowable strain of 0.01% for annealed glass and 2% for FT glass panels before fracture as well as a maximum deflection of 8 mm (0.315") for fully-tempered glass and only 2 mm (0.079") for annealed glass panels prior to shattering.

The element deletion method is more advantageous compared to the earlier yield-line analysis as it actually removes the failed elements in each time step and recalculates and re-constructs the stiffness, mass and force matrices for the next time increment. Therefore, the stress values across the panel at each time frame are a true representation of the real stress state in the glass panel: As more elements reach their failure and get removed from the geometry, this computational technique takes into account the stress concentrations at the crack tips as well as the real stress wave distribution paths across the panel.

Moreover, as the element deletion technique also follows the crack path through removal of the failed elements, the crack branching and propagation is therefore the true representation of the actual glass panel behavior when subjected to an explosive event. Furthermore, the failure times in the element deletion technique are real: meaning that the real-life pre and post-crack behavior of the glass panels can be traced and reported with greater accuracy and confidence.

VI. FAILURE PATTERNS OF HOMOGENEOUS WINDOW PANELS

The calculated failure pattern of conventional homogeneous 50 cm x 75 cm annealed glass window panels, subjected to small intensity air blast, is illustrated in Fig. 3 (below). The stress contours in the corners rise at 2.5 msec and the stress waves

DOI: 10.5963/AMSA0303002

find their way towards the panel center at 4.175 msec. Then, at 4.75 msec, the glass panel cracks in the middle along the vertical yield line and therefore, the crack propagates towards the upper and lower boundaries. Thereafter, as predicted by the yield-line analysis, the cracks expand towards the corners at 6.75 msec followed by the total glass panel failure at 12.00 msec.

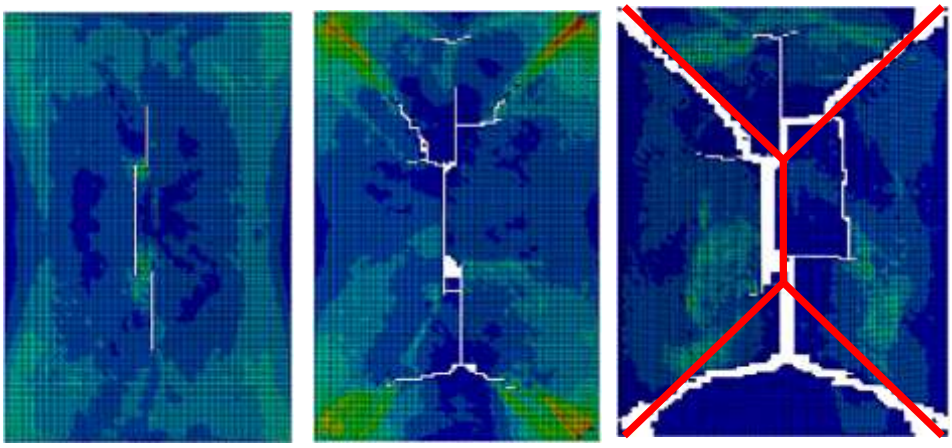

Fig. 3 Stress distribution and crack propagation patterns for conventional homogeneous AG panels subjected to smaller intensity air blast: (left) 4.75 msec, (center) 6.75 msec, (right) 12.00 msec

Failure pattern of conventional homogeneous annealed glass window panels subjected to higher intensity air blast is illustrated in Fig. 4. In this case, compared to the case of smaller blast, the stress contours across the panel rise with faster pace and the stress waves find their way towards the panel center where a higher crack accumulation will be formed. The glass panel cracks in the middle at 3.75 msec and the cracks propagate towards the corners at 4.25 msec followed by the total panel failure that happens at 5.85 msec in compliance with the pattern predicted by the yield line analysis.

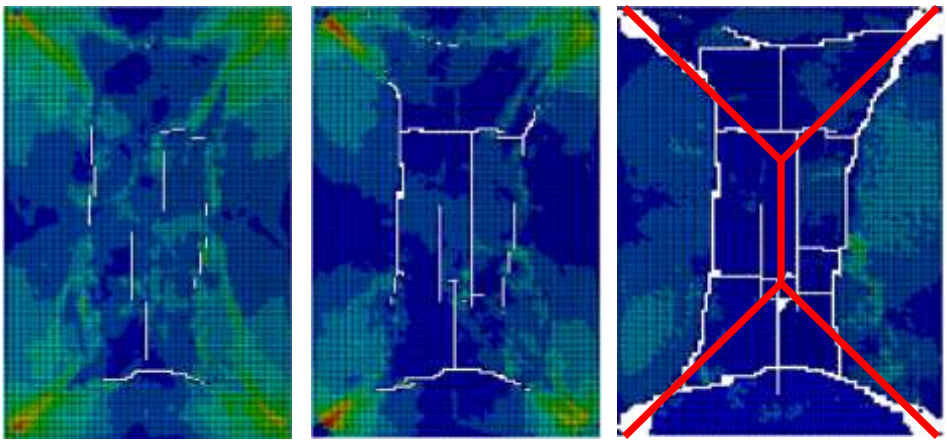

Fig. 4 Stress distribution and crack propagation patterns for conventional homogeneous AG panels subjected to higher intensity air blast: (left) 3.75 msec, (center) 4.25 msec, (right) 5.85 msec

Fig. 5 also demonstrates the failure pattern of conventional simply-supported homogeneous FT glass panels subjected to higher intensity air blast. The longitudinal vertical crack that appears at 8.875 msec will start branching further at 11.363 msec. Thereafter, other horizontal and vertical cracks will be formed across the panel that eventually will divide the panel into smaller blocks and fragments, as the dominant failure pattern, at 12.975 msec.

DOI: 10.5963/AMSA0303002

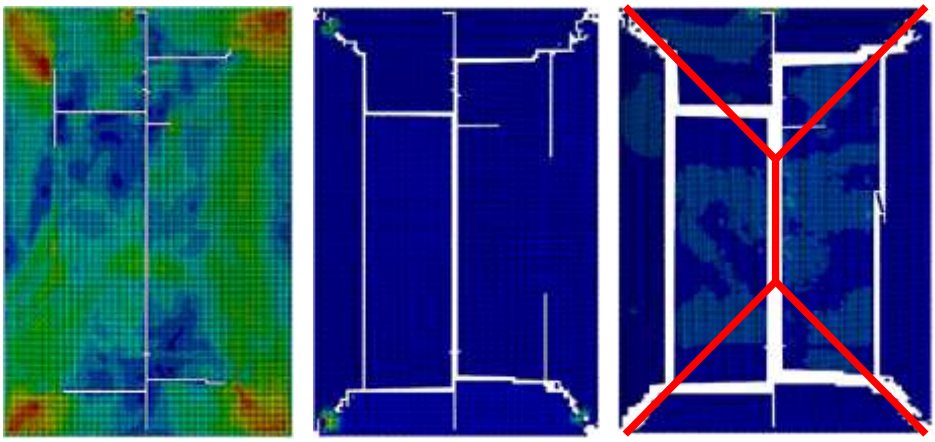

Fig. 5 Stress distribution and crack propagation patterns for conventional homogeneous FT panels subjected to higher intensity air blast: (left) 8.875 msec, (center) 11.363 msec, (right) 12.975 msec

VII. PANEL DEFECTS AND NON-HOMOGENEITY EFFECT ON FAILURE PATTERNS

ASTM C1036 (2011) [18] categorizes major glass defects for annealed glass with Quality – Q4 (general glazing applications) as crush (lightly pitted condition with a dull gray appearance); dig (deep short scratch); knot (inhomogeneity in the form of a vitrous lump); dirt (inclusion of small foreign matter particle in the surface of flat glass); gaseous inclusion (entrapped air bubbles); stone (crystalline inclusion in glass); blemishes (imperfections in the glass body or surface); scratches (damage to the glass surface due to the movement of a foreign object against it); as well as shell chips (circular indentation in the glass edge); and v-chips that are v-shaped imperfections in the edge of the glass lite. Furthermore, according to the ASTM C1036 (2011) [18] guidelines, annealed glass panels with a thickness of 6 mm (1⁄4") or less shall not vary in thickness more than 0.1 mm (0.004") over a 100 mm (4") length.

Imperfections of fully-tempered glass panels, according to ASTM C1048 (2012) [19], are commonly the following: curvature warps across either one or both panel dimensions; crush; dig (deep short scratches); small particle of foreign matter (sand or other imperfections on the roller surface during the heating or cooling procedure); distortion due to heating; air bubble inclusions; scratches and holes. As demonstrated in Fig. 6 (below), the FT panel holes need to have a minimum distance of the greater value of 6 mm (1/4") or two times of panel thickness from any panel edge as well as greater of 10 mm (3/8") or twice of thickness from the adjacent hole rim. Minimum diameter of the holes should also be greater of either 6 mm (1/4") or the panel thickness.

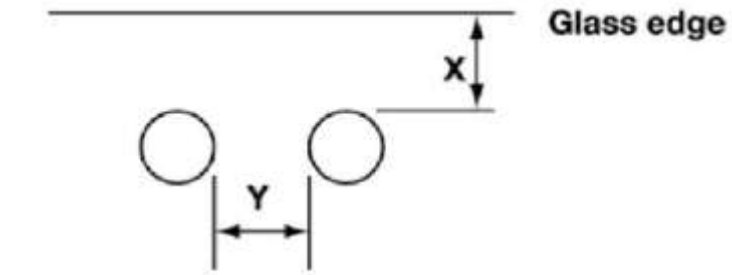

Fig. 6 Placement of holes across the FT glass panel according to ASTM C1048-12

Moreover, ASTM C1048 (2012) [19], indicates that the surface and edge compression tests on fully tempered glass panels should be performed twice on each of the five locations illustrated in Fig. 7 where *L* is the window panel length and *W* is the width of the panel.

DOI: 10.5963/AMSA0303002

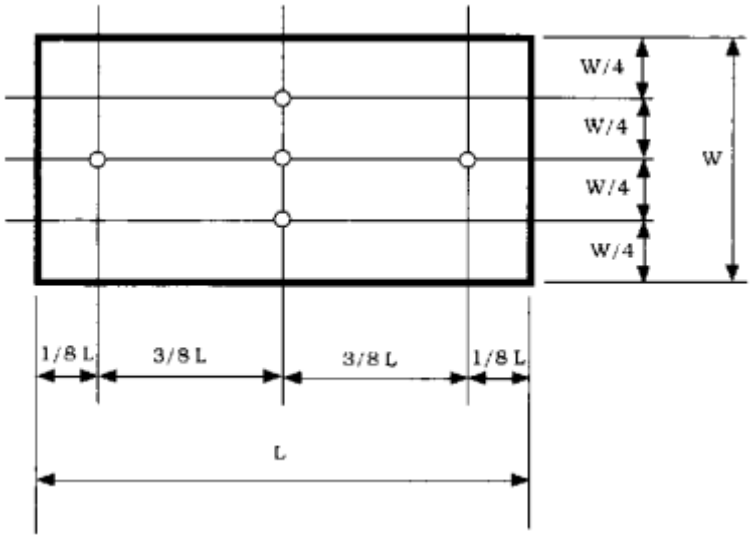

Fig. 7 Five Location Examination for Fully Tempered Glass Panels (ASTM C1048-12)

In this paper, the effects of two most common defect categories on failure patterns of the proposed simply-supported 50 cm x 75 cm window panels have been investigated and compared. For the annealed glass panels, the existence of two chips in the right-hand-side and upper-left edges of the panels according to ASTM C1036 (2011) [18] and subjected to both small and higher intensity air blasts is investigated. The existence of three individual holes (air inclusions during the manufacturing process) in compliance with ASTM C1048 [19] five-point examination locations is also investigated for the fully-tempered glass panels that are subjected to higher intensity air blasts.

The schematic view of the defective annealed and fully-tempered window panels that are studied in this paper along with their types and locations is demonstrated in Fig. 8.

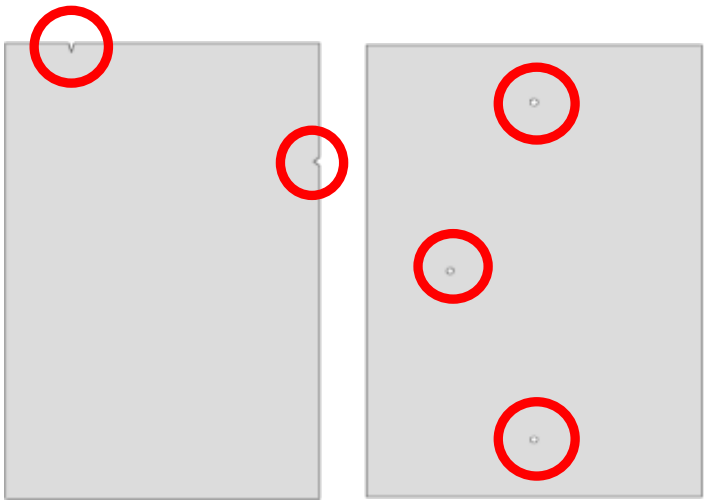

Fig. 8 (Left) Existence of chips in the annealed glass (AG) panel edges, (Right) Location of the holes across the fully-tempered (FT) glass window panel

Fig. 9 illustrates the crack propagation path for defective conventional annealed glass panels that are subjected to small intensity air blast. The window panel center starts cracking at 4.362 msec and, as it is seen in the Figure, the crack propagates vertically at 5.325 msec with maximum stress lines passing through the corners and the upper-left chip. Due to the weakness of the panel in the right side, the bottom corner will come off at 7.050 msec (while the crack path is in general agreement with the yield line analysis). The panel will then fail at 8.725 msec which occurs faster compared to the case of homogeneous AG panel with a failure time of 12.00 msec.

DOI: 10.5963/AMSA0303002

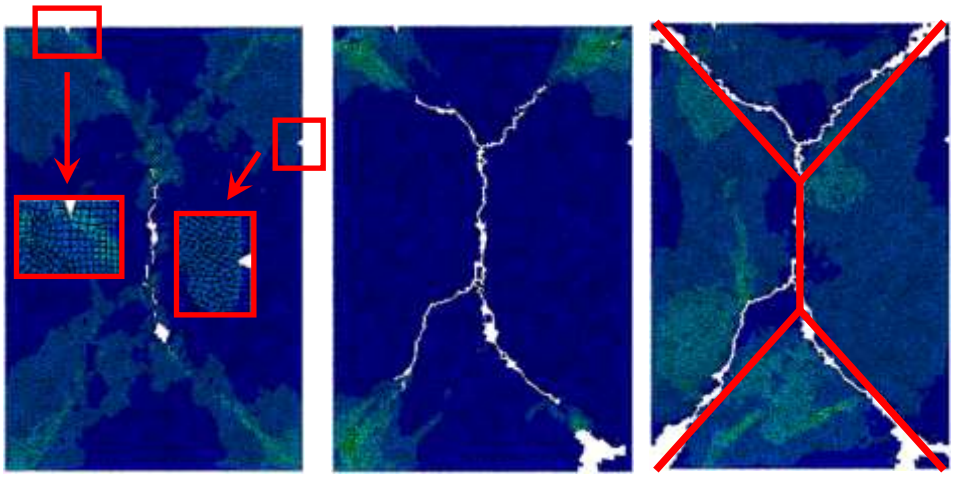

Fig. 9 Stress distribution and crack propagation patterns for conventional defective AG panels subjected to smaller intensity air blast: (left) 5.325 msec, (center) 7.050 msec, (right) 8.725 msec

Therefore, as it is illustrated in the Figure, the general failure pattern of the annealed glass panel with chips at the edges will be similar to that of the homogeneous panel; however having less symmetric pattern and happening at a much faster pace.

Fig. 10 demonstrates the crack propagation path for conventional annealed glass panels that are subjected to higher intensity air blast. As it is seen in the Figure, the failure pattern of the glass panel will be very similar to the case of small-intensity air blast. However, in this case, the higher severity of the blast loading will cause the large rotation angles in the elements that will eventually lead to computational instability at the time of glass failure at 6.518 msec.

The imperfection locations, therefore, will have minor effect on general failure pattern of the annealed glass panels that are subjected to higher intensity air blast. The general failure pattern of the panels will be more in accordance with the yield line analysis predictions. Furthermore, the glass panel failure will happen faster (compared to the case of smaller intensity air blast).

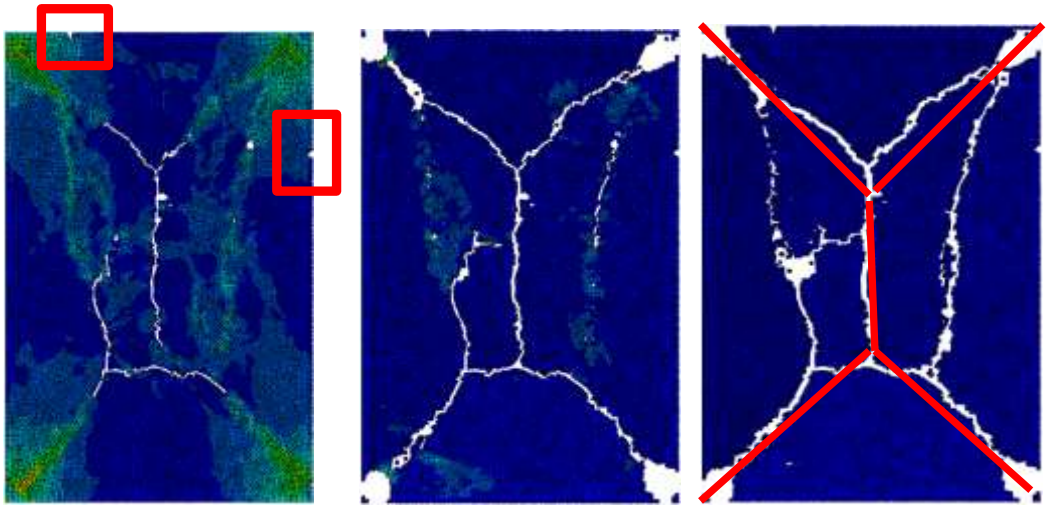

Fig. 10 Stress distribution and crack propagation patterns for conventional non-homogeneous AG panels subjected to higher intensity air blast: (left) 3.812 msec, (center) 5.475 msec, (right) 6.518 msec

Fig. 11 shows the crack propagation path and failure pattern of defective conventional 50 cm x 75 cm fully tempered glass windows with three holes (air inclusions) across the panel that are located in accordance with the five examination points locations as per ASTM C1048 (2012) [19] guidelines (demonstrated in Fig. 7).

DOI: 10.5963/AMSA0303002

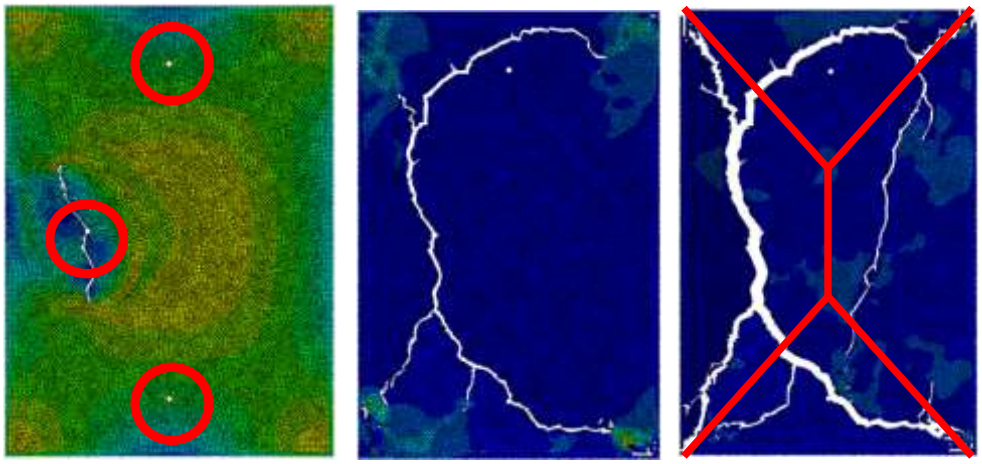

Fig. 11 Stress distribution and crack propagation patterns for conventional defective FT panels subjected to higher intensity air blast: (left) 4.60 msec, (center) 7.787 msec, (right) 9.90 msec

Subjected to higher intensity air blast, stress contours across the fully-tempered glass panels rise in the corners and the center, where, due to the glass defect location eccentricity, the first crack initiates in the panel center at 4.57 msec and propagates vertically at 4.60 msec. This is particularly due to the excessive stress concentrations at the location of the middle hole as well as the high brittleness of the tempered glass. Thereafter, the crack path passes through the second imperfection location as another panel weak point at 4.70 msec. From there, cracks find their way towards the panel corners at 7.787 msec (as seen in the Figure) until the complete panel failure time at 9.90 msec. The total failure in the panels with imperfections occurs faster in comparison with the homogeneous fully tempered glass panel failure that happens at 12.975 msec.

VIII. SUMMARY AND CONCLUSIONS

In this paper, the failure patterns of homogeneous and defective glass window panels for two different types of glazing systems (annealed and fully-tempered glass panels) subjected to two different air blast intensities are investigated and compared. The required blast overpressure amount for window panel breakage for both annealed glass and fully-tempered glass panels is calculated using the yield line analysis to predict whether the failure will occur in each of the proposed glazing system technologies and the air blast intensities.

In order to envisage the crack paths and obtain the panel failure time histories, explicit finite element simulation along with element-removal technique is adopted for modeling the conventionally-framed (simply-supported) window panel failures. This computational technique follows the crack path through removal of the failed elements and stress redistributions at each infinitesimal time increment to demonstrate the brittle failure behavior of the window glass panels.

The existence of imperfections across the glass window panels will make them more vulnerable against the air blast overpressures for both annealed and fully-tempered glass panel cases. For fully tempered glass panels, the vulnerability arises from greater stress concentrations at the location of glass defects (air inclusions) as well as the higher brittleness of the panel itself when compared to the annealed glass panels. In the fully-tempered panels, when subjected to higher air blast intensities, the cracks will initiate at the location of the imperfection (air inclusion holes) in the middle of the panel where the stress contours are at their highest and thereafter propagate towards other defect locations (the second air bubble inclusion location, for instance).

For the case of annealed glass panels, however, the existence of the defects (chips) along the edges will help in redistribution of the stresses in such a way that the yield lines will pass through these imperfection locations. Therefore, subjected to smaller-intensity air blast, the general failure pattern of these annealed glass panels will be very similar to that of the homogeneous window panels yet with a faster pace. In annealed glass panels that are subjected to medium intensity air blast, the severity of the load will cause excessive rotation angles in the finite element model and thus a subsequent computational divergence and instability will occur in re-meshing of the post-cracked glass panel. In these panels, when compared to the case of smaller-intensity air blasts, the panel failure will demonstrate a different pattern and will occur in a much accelerated pace.

For conventional glass window panels (simply-supported), balancing the safety and security of the window panels with physical appearance and cost-effectiveness requires a better understanding of the glass panel responses to different characteristics of the glazing system technologies and the blast load parameters. Such analysis and modeling will help in developing more comprehensive flying glass injury models that address the appropriate structural, architectural and building envelope choices to mitigate the threats facing the safety of the building occupants during an air blast.

DOI: 10.5963/AMSA0303002

REFERENCES

[1] E. Trawinski, J.W. Fisher, and R.J. Dinan, "Full scale testing of polymer reinforced blast resistant windows," *Air Force Research Laboratory Report*, AFRL-ML-TY-TP-2005-4508, Florida, USA, 2004.

[2] H.S. Norville, N. Harvil, E.J. Conrath, S. Shariat, and S. Mallonee, "Glass- related injuries in Oklahoma," *ASCE Journal of Performance of Constructed Facilities*, vol. 13(2), pp. 50-56, 1999.

[3] N.F. Johnson, "International Standards for Blast Resistant Glazing," *Journal of ASTM International*, vol. 3, no. 4, 2006.

[4] H. Ataei and J.C. Anderson, "Computational Modeling of Glass Panels for Mitigating the Injuries due to Air Blast," *Proceedings of 2013 ASCE International Workshop of Computing in Civil Engineering*, pp. 57-64, 2013.

[5] T. Belytscheko, W.K. Liu, and B. Moran, *Nonlinear Finite Element for Continua and Structures*, John Wiley and Sons Ltd., 2005.

[6] H. Ataei, J.C. Anderson, and A. M. Niazy, "Resistance of Glass Panels to Air Blast," *Proceedings of PROTECT2007 International Congress*, Vancouver, BC, Canada, 2007.

[7] ABAQUS (2011), "ABAQUS Documentation," Dassault Systèmes, Providence, RI, USA.

[8] H. Ataei H. and J.C. Anderson, "Mitigating the Injuries from Flying Glass due to Air Blast," *Proceedings of ASCE 6th Congress on Forensic Engineering*, pp. 133-142, 2012.

[9] ASTM Standard F1642-04, (2010), "Standard Test Method for Glazing and Glazing Systems Subject to Airblast Loadings," ASTM International, West Conshohocken, PA, USA, 2010.

[10] A. Ingerslev, "The Strength of Rectangular Slabs," *The Journal of the Institute of Structural Engineers*, vol. 1, no. 1, 1923.

[11] E. Hognestad, "Yield Line Theory for Ultimate Flexural Strength of Reinforced Concrete Slabs," *Proceedings of American Concrete Institute*, vol. 24, pp. 637-656, 1953.

[12] E.G. Nawy, *Reinforced Concrete: A Fundamental Approach*, 4th Edition, Prentice Hall, Upper Saddle River, NJ, 2000.

[13] J.N. Reddy, *Theory and Analysis of Elastic Plates and Shells*, 2nd Edition, CRC Press, 2006.

[14] R. Park and W.L. Gamble, *Reinforced Concrete Slabs*, 2nd Edition, John Wiley & Sons, 2000.

[15] ASTM Standard E2461 - 05, (2011), "Standard Practice for Determining the Thickness of Glass in Airport Traffic Control Tower Cabs," ASTM International, West Conshohocken, PA, USA, 2011.

[16] Canadian GSB Publication CAN/CGSB-12.20-M89, (1989), "Structural design of glass for buildings," Canadian General Standards Board, Gatineau, Canada, 1989.

[17] P. Kumar P. and A Shukla A., "Dynamic Response of Glass Panels Subjected to Shock Loading," *Journal of Non-Crystalline Solids*, vol. 357, pp. 3917-3923, 2011.

[18] ASTM Standard C1036 – 11, (2011), "Standard Specification for Flat Glass," ASTM International, West Conshohocken, PA, USA, 2011.

[19] ASTM Standard C1048 – 12, (2012), "Standard Specification for Heat-Strengthened and Fully Tempered Flat Glass," ASTM International, West Conshohocken, PA, USA, 2012.

Hossein Ataei is a registered Professional Engineer and is currently teaching engineering courses at the California State University. He has a PhD in civil engineering from University of Southern California (USC) in Los Angeles, USA. In addition, he holds two Masters degrees in Construction Management and in Business Administration. He has worked in structural design and the project management of large civil infrastructure projects.

James C. Anderson is a distinguished professor of civil and structural engineering at the University of Southern California (USC) in Los Angeles, USA. He has a PhD in civil engineering from University of California, Berkeley. His works in the fields of structural engineering; earthquake engineering and performance-based design are published as books, book chapters, journal papers, conference publications and technical reviews both internationally and in the United States.

DOI: 10.5963/AMSA0303002